LATVIAN JOURNAL OF PHYSICS AND TECHNICAL SCIENCES
2017, N 6

DOI: 10.1515/lpts-2017-0040

PERFORMANCE EVALUATION OF IRBENE RT-16 RADIO TELESCOPE RECEIVING SYSTEM

M. Bleiders, Vl. Bezrukovs, A. Orbidans
Engineering Research Institute "Ventspils International Radio Astronomy Center" of Ventspils University College, Inzenieru str., 101, Ventspils, LV-3601, LATVIA

In the present paper, recent measurement results of refurbished Irbene RT-16 radio telescope receiving system performance are presented. The aim of the research is to evaluate characteristics of RT-16, which will allow carrying out necessary amplitude calibration in both single dish and VLBI observations, to improve the performance of existing system as well as to monitor, control and compare performance if possible changes in the receiving system will occur in future. The evaluated receiving system is 16 m Cassegrain antenna equipped with a cryogenic receiver with frequency range from 4.5 to 8.8 GHz, which is divided into four sub-bands. Multiple calibration sessions have been carried out by observing stable astronomical sources with known flux density by using in-house made total power registration backend. First, pointing offset calibration has been carried out and pointing model coefficients calculated and applied. Then, amplitude calibration, namely antenna sensitivity, calibration diode equivalent flux density and gain curve measurements have been carried out by observing calibration sources at different antenna elevations at each of the receiver sub-bands. Beam patterns have also been evaluated at different frequency bands. As a whole, acquired data will serve as a reference point for comparison in future performance evaluation of RT-16.

Keywords*: amplitude calibration, pointing calibration, radio astronomy*

1. INTRODUCTION

Ventspils International Radio Astronomy Centre (VIRAC) radio telescope RT-16 at Irbene has recently been upgraded with new mirror, tracking and reception systems, which have already been verified in multiple astronomical observations during the year 2017, including successful Very Long Baseline Interferometric (VLBI) sessions in European VLBI Network (EVN), and multiple types of single dish observations, including Active Galactic Nucleus (AGN) and spectral line monitoring. To improve the performance of RT-16 in both VLBI and single dish modes, multiple calibration sessions have been carried of which the main results are described in subsequent sections. First of all, evaluation and compensation of beam pointing errors have been carried out. Secondly, optimum feed horn position at secondary focus has been found. Then, the main characteristic parameters of radio telescope have been

evaluated, which include antenna gain elevation dependence, system temperature and beam patterns. Performance has been evaluated at frequencies of 4.5 to 8.8 GHz, which is frequency range of RT-16 main receiver divided into four sub-bands that are designated as C1 to C4 in this paper. For the reference, the main parameters of RT-16 system are summarized in Table 1.

Table 1

Summary of RT-16 Radio Telescope System

REFLECTOR SYSTEM	
Diameter of primary mirror	16 m
Diameter of secondary mirror	1.6 m
Distance of primary base to secondary focus	2.095 m
f/D of primary mirror	0.3
Subtended angle at secondary focus	34°
Surface error of primary mirror	635 μm RMS [6]
Half power beam width	C1: 0.26° or 16 arcmin, C2: 0.21° or 13 arcmin C3: 0.20° or 12 arcmin, C4: 0.16° or 10 arcmin
TRACKING SYSTEM	
Az/El range	-328 to +328° / 2.5 to 94°
Az/El maximum velocity	5/4 °/s
Az/El maximum acceleration	1.5/2 °/s/s
Az/El tracking accuracy	3.3 arcsec /3.3 arcsec
RECEIVER SYSTEM	
Frequency range	4.5 to 8.8 GHz
Frequency ranges of available sub-bands and frequency of corresponding local oscillator	C1: 4500 – 5500 MHz, LO = 4100 MHz C2: 5400 – 6400 MHz, LO = 5000 MHz C3: 6400 – 7600 MHz, LO = 6100 MHz C4: 7600 – 8800 MHz, LO = 7300 MHz
Polarization	Right and Left Circular Polarizations
Calibration functionality	Noise source injection and VLBI phase cal. system
Available signal registration back-ends	DBBC2/Mark5c, Total power meter and Spectrum analyzer

2. CALIBRATION OF POINTING ERRORS

Before it is possible to carry out any observations, it is necessary to characterize pointing errors because it is not possible to rely solely on constant tracking system encoder offsets due to potential secondary mirror or feed displacements, gravitational deformations, axis misalignment etc. which may also be dependent on antenna elevation and azimuth. To characterize pointing errors, multiple applications included in VLBI Field System (FS) were employed [1] in combination with in-house made total power meter which was integrated in FS as a station detector for this purpose. Measurements were carried out mostly in C3 band (see Table 1) with bandwidth of 1200 MHz as it was reasonably high frequency and clean from radio

interference. To measure pointing offsets at particular antenna position, application FIVPT was used, which implemented discrete point cross-scans in both azimuth and elevation axis across the astronomical point source and linear-Gaussian function fitting algorithm to calculate offsets.

Multiple 12 to 24 hour long pointing calibration sessions were carried out to acquire pointing offsets at different antenna position angles by cross-scanning bright point sources 3C123, 3C84, 3C461 (CasA), 3C405 (CygA), 3C144 (TaurusA), 3C145 (OrionA) and 3C454.3. For data acquisition control FS AQUIR application was used. Here we present results of recent calibration session, carried on 28 July, 2017. Total of 213 points were acquired with sky coverage shown in Fig. 2. For more uniform coverage a source list must be increased, which may not be feasible with a current cross-scan algorithm because source fluxes may be too weak in case of RT-16 to obtain reliable results. Weather conditions during the session were good, with clear sky and low wind.

To compensate for azimuth and elevation dependent pointing offsets, the model is fit on the raw offset data, which afterwards is used to calculate offset at any antenna position. In this case, we were employing FS pointing model, which was based on 23 antenna physical parameter model described in [2]. To obtain parameters of the model FS PDPLT application was used. Results together with raw data are visualized in Fig. 1.

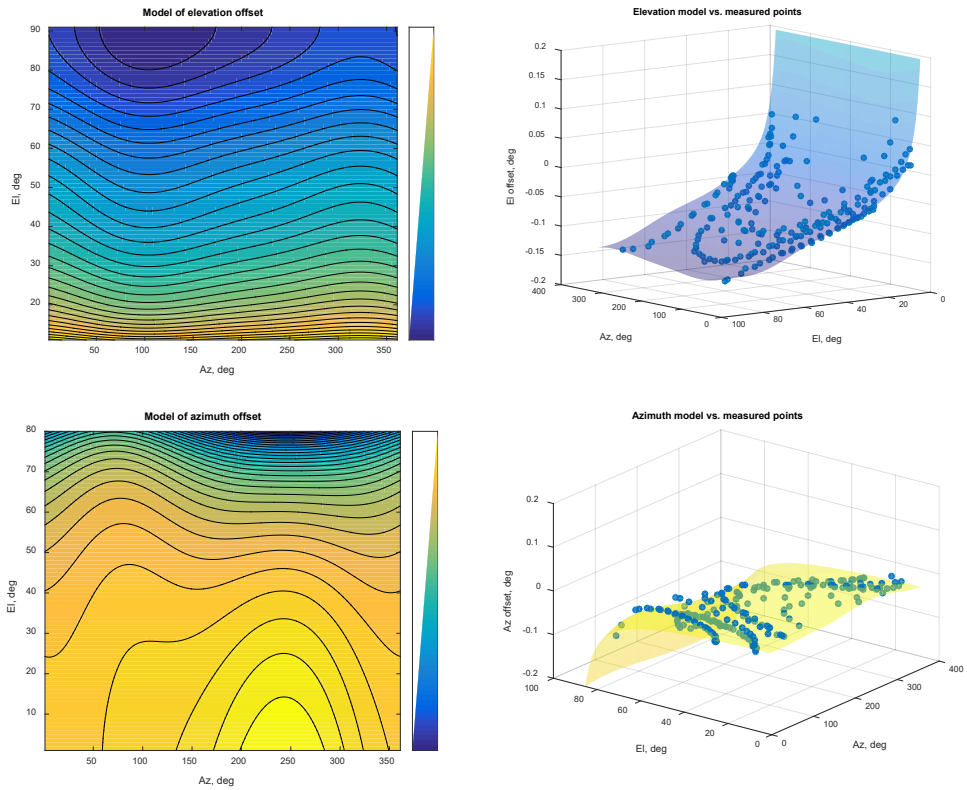

Fig. 1. Derived pointing models of RT-16 and raw data points (28 July, 2017).

There is relatively large elevation offset dependence on elevation present with maximum amplitude of ≈0.15° which is almost 100 % of Half Power Beam Width (HPBW) at highest frequency band (C4 – 8400 MHz) of RT-16. It may be explained with possible secondary mirror gravitational sag, which is also evident in antenna beam patterns (see Fig. 9) In the case of azimuth offsets, dependence on elevation and azimuth is relatively flat up to elevations of ≈65° where at higher angles offsets start to increase. Interestingly, there is some kind of hysteresis present, which can be noticed in bottom right plot of Fig. 1. In other words, at higher elevations, azimuth offset values differ at almost the same azimuth and elevation positions – the only known difference is being direction of antenna slew for those points. Due to this issue and combination with small sky coverage at higher elevations, accuracy of azimuth model is poor above elevations of 70° and must be investigated more thoroughly. Overall statistics of current pointing model are shown in Table 2. Pointing model was verified by carrying out successive calibrations session, results of which could be compared in Fig. 2 and Fig. 3.

Table 2

Residuals of Pointing Model Shown in Fig. 1

Azimuth RMS residual: 0.015° (54”), Max error: 0.039° (140”)
Elevation RMS residual: 0.0065° (23.4”), Max error: 0.021° (76”)

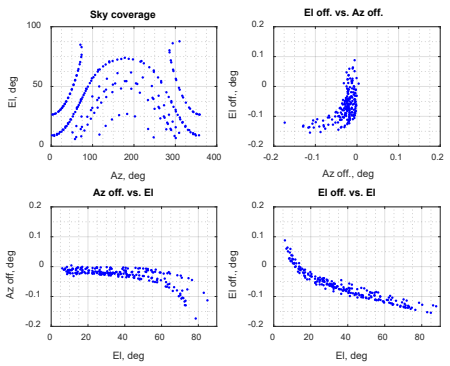

Fig. 2. Pointing errors of RT-16 before applying the pointing model.

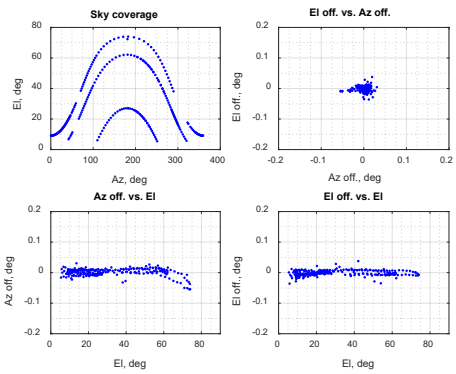

Fig. 3. Pointing errors of RT-16 after applying the pointing model.

3. BASICS OF AMPLITUDE CALIBRATION

In general, radio telescope amplitude calibration can be described using following equations [3]:

$$Tcal[Jy] = S_f[Jy] \cdot \frac{TP_{cal} - TP_{sky}}{TP_{src} - TP_{sky}} \quad (1)$$

$$Tcal[Jy] = \frac{Tcal}{DPFU(El)} \cdot e^{\tau * AM} \quad (2)$$

$Tcal[Jy]$ - Calibration diode noise in Jy;

$S_f[Jy]$ - Source flux density in Jy. Assumed to be constant and known;

TP_{cal} - Measured power with beam off source and cal. diode on;

TP_{sky} - Measured power with beam off source and cal. diode off;

TP_{src} - Measured power with beam on source and cal. diode off;

$Tcal$ - Cal. diode noise density in K. Assumed to be constant and known;

$DPFU(El)$ - Elevation dependent antenna gain in Degrees Per Flux Units, K/Jy;

τ - Atmospheric zenith opacity;

AM - Air mass coefficient. $AM \approx \frac{1}{\sin(El)}$.

Calibration noise equivalent flux density *Tcal[Jy]* can be directly measured, by comparing total power increment caused by injected noise diode signal and observed source with known flux. *Tcal[Jy]* is dependent on calibration noise source signal power and antenna gain, which can be calculated using (2), if calibration diode noise density in Kelvins is known. Depending on observation frequency and weather conditions atmospheric absorption term $e^{\tau * AM}$ has to be taken into to account. In case of relatively low available frequencies of RT-16 receiver, atmospheric absorption becomes noteworthy only at elevations below ≈10°, but attention should be devoted if observing in C4 band and/or weather conditions are not optimal. Basically, one only needs to know *Tcal[Jy]* to calibrate raw data to absolute flux units, but separating the system noise and gain from the equation (see (3), (4)) is useful for characterizing and monitoring the antenna and receiver subsystems of telescope separately.

4. DETERMINATION OF OPTIMAL FEED HORN POSITION

RT-16 C band receiver includes a linear actuator system which allows axially moving the feed horn assembly in total range of 650 mm to fine tune its position in secondary focus and facilitate the maintenance. Although optimum position of the feed was already roughly known, more accurate measurement was carried out. 6.7 GHz methanol maser W3OH was chosen as a reference source for gain measurement, which increased measurement accuracy and speed, because signal amplitude could be measured without physically moving the beam off the source. Measurement was carried out with automated read-back of spectrum analyzer marker values while tracking the source and at the same time moving the feed horn from lower position at 0 to upper position at 650 mm. To calibrate receiver gain variations, calibration noise diode was switched during the measurement. Signal spectrum during the measurement process and equations used for gain calculation are outlined in Fig. 4. Marker M1 represents the on-source signal – automatic peak tracking was turned on for M1 to compensate for any Doppler shift during the measurement which might be significant if similar measurement were carried out in timescales of few hours. Average of M2 and M3 represents the off-source signal and frequency positions these markers were chosen experimentally to be maximally close to the spectral line. Total measurement time was 11 minutes which was limited by actuator movement speed and

total elevation change during the measurement was only from 38° to 37° so elevation dependence of gain and system temperature could be neglected. System temperature and gain (in form of DPFU) were calculated according to equations (3), (4) derived from rearranging (1), (2). Results are shown in Fig. 5.

$$T_{sys} = T_{cal} \cdot \frac{TP_{sky}}{TP_{cal} - TP_{sky}} \tag{3}$$

$$DPFU = \frac{T_{sys}}{S_f} \cdot \frac{TP_{src} - TP_{sky}}{TP_{sky}} \tag{4}$$

T_{sys} - system temperature, K;
$DPFU$ - gain, K/Jy;
T_{cal} - calibration noise temperature, K;
S_f - calibration source flux, Jy;
TP_{cal} - <M2,M3> with cal diode on;
TP_{sky} - <M2,M3> with cal diode off;
TP_{src} - M1 with cal diode off.

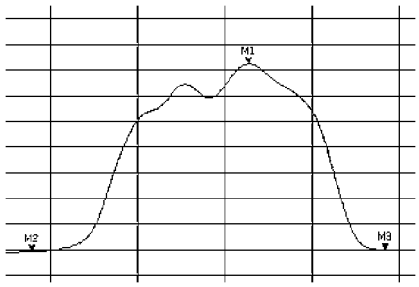

Fig. 4. Gain measurement using methanol spectral line W3OH source.

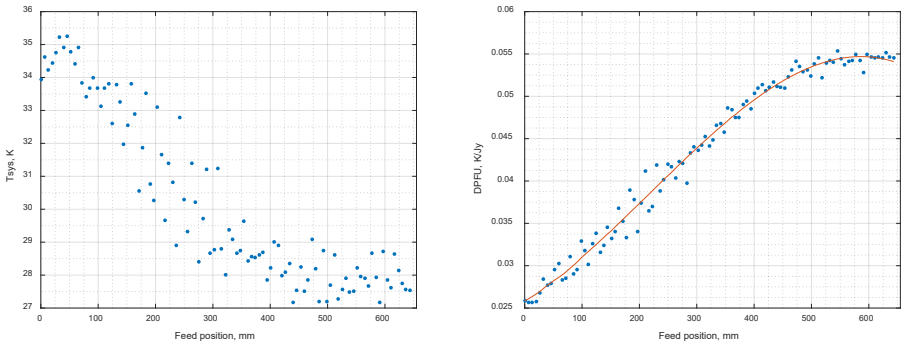

Fig. 5. System temperature and DPFU dependence on axial position of RT-16 feed antenna measured at 6700 MHz.

Measurement results show that not only DPFU varies with feed position, but also decreases when feed is in upper position which could be explained with less noise pickup from secondary cone walls in comparison with case when feed is fully

shifted inside the cone. Right graph of Fig. 5 shows that maximum gain is reached when feed is at 650 mm position and judging from flatness of the response at that point, this is the optimum position. It should be noted that this measurement was carried only at 6.7 GHz due to availability of spectral line sources. For maximum confidence, similar measurements would have to be carried out at rest of the sub-bands to determine if any compensation were needed due to frequency dependence of feed antenna phase center position, probably using ONOFF method and continuum sources. However, seeing the flat response at the focus point at 6.7 GHz, gain loss due to a focusing error at lower frequency bands should not be much increased.

5. MEASUREMENT OF ANTENNA GAIN

To determine the antenna gain of RT-16 at different sub bands and more importantly its dependence on elevation or gain curves, position switched measurement procedure based application ONOFF provided by FS was used for measurement of *Tcal[Jy]* from which the gain in form of DPFU was derived using (2). Multiple calibration sessions were carried out to measure gain at all four sub bands and both polarization channels. Total power measurement was carried out in full bandwidth of the sub-band (≈1200 MHz). FS AQUIR application was used to collect the data at different antenna elevations by observing sources with the known flux density. Sources 3C123, 3C196, 3C295, 3C286 were used as flux calibrators with flux scales adapted from [5]. As an exception, 3C84 was used at measurement of gain curve at C4 band because of its relatively high brightness which allowed decreasing the scatter of the data. Weather conditions during the measurements were good, with clear sky, expect it was overcast during the C4 band measurement. During the measurement, the pointing model described previously was applied. No opacity corrections were applied. Example of measurement results together with raw data points for C1 are shown in Figure 6 and curves for all bands are shown in to Figure 7. Third order polynomial function was fit on the measured data points and could be used to calculate elevation dependent DPFU in (2) using (5). Polynomial coefficients for all sub bands are shown in Table 3.

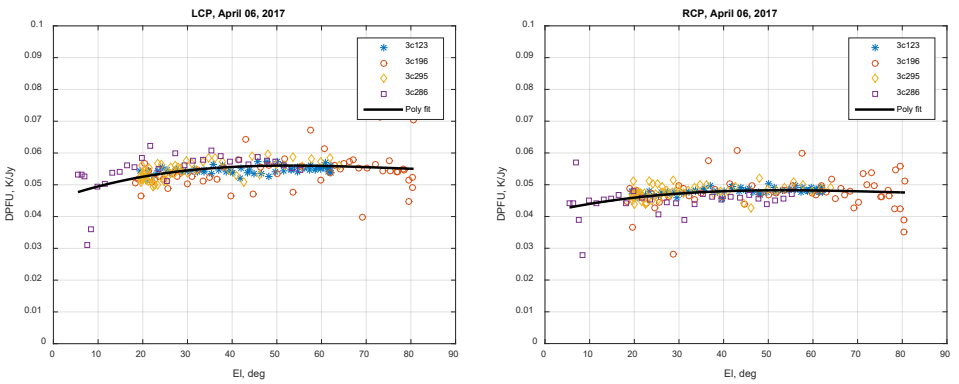

Fig. 6. DPFU dependence on elevation at C1 (5000 MHz) sub band.

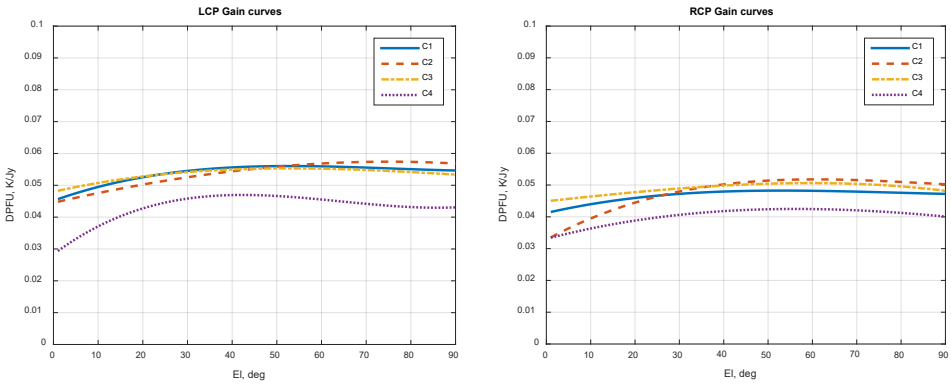

Fig. 7. Gain polynomial curves for C1 to C4 sub-bands.

$$DPFU(El) = DPFU \cdot (a_3 \cdot El^3 + a_2 \cdot El^2 + a_1 \cdot El + a_0) \quad (5)$$

Table 3

Gain Curve Polynomial Coefficients for RT-16 at C1 to C4 Sub-bands

Sub b.	Pol	T_{cal}, K	DPFU, K/Jy	a_3	a_2	a_1	a_0
C1	RCP	50.34	0.0484	3.94E-07	-8.20E-05	5.36E-03	8.88E-01
	LCP	50.34	0.0550	1.50E-07	-3.57E-05	2.61E-03	9.40E-01
C2	RCP	45.01	0.0510	1.38E-06	-2.66E-04	1.59E-02	6.95E-01
	LCP	45.01	0.0552	-1.15E-07	-6.22E-06	2.19E-03	9.15E-01
C3	RCP	41.29	0.0506	-2.23E-07	-5.26E-06	3.00E-03	8.87E-01
	LCP	41.29	0.0553	2.48E-07	-7.39E-05	5.73E-03	8.67E-01
C4	RCP	31.16	0.0432	6.20E-07	-1.67E-04	1.24E-02	7.20E-01
	LCP	31.16	0.0479	2.58E-06	-4.14E-04	1.96E-02	7.03E-01

The obtained gain curves are relatively flat at all bands which are expected from light antenna surface and relatively low frequencies of RT-16 C band receiver. No pronounced maximum is present, but gain tends to increase at higher elevations which may be explained by fact that panels of primary surface were adjusted in zenith position. Consistently increased DPFU is observed in LCP channel at all bands, which may be a result of inaccurate values which were assumed to be the same for both polarization channels and must be determined in the future using hot-cold absorber calibration. No major absolute value differences are present between the sub-bands, expect for the C4 where reduced gain was observed, which should be verified after calibration of .

6. SYSTEM TEMPERATURE AND OPACITY

Additional outcome of ONOFF measurement is system temperature T_{sys} which can be calculated using (3). As absolute values are highly dependent on weather conditions and knowledge of T_{cal}, the following data should be considered as approximate and is useful for relative comparison only. Elevation dependence of T_{sys}

at different sub-bands were measured during the amplitude calibration sessions described in last section and example for C1, C4 sub bands is shown in Fig. 8.

It can be noticed that absolute values of T_{sys} are different between polarization channels which may be due to insufficient knowledge of T_{cal}. In all sub bands response is relatively flat down to elevations of ≈45°, where it starts to increase due to increase of atmosphere absorption and antenna spillover. Data of T_{sys} elevation dependence or the so called "skydip" measurement allows calculating zenith opacity τ which can be used to compensate atmospheric absorption according to (2). Steps of determining the opacity are outlined in [3] and [5]. Table 4 shows opacity determined from data shown in Fig. 8. Value shown for each sub band is average between both polarization channels. Opacity is increasing with increasing frequency as it is expected, but more frequent measurement should be carried to conclude if atmospheric absorption should be compensated in RT-16 C band astronomical data.

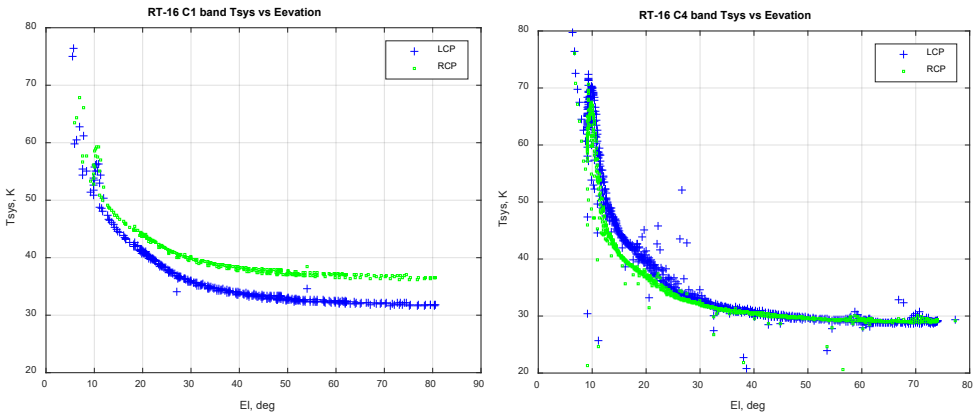

Fig. 8. Elevation dependence of RT-16 system temperature at C1, C4 sub-bands.

Table 4

Zenith Opacities at Different Sub-bands Measured during April to August, 2017. Weather Conditions: Clear Skies Expect Overcast in C4 Sub-band

Sub-band	C1 5000 MHz	C2 6100 MHz	C3 6700 MHz	C4 8400 MHz
Zenith opacity	0.0156	0.0163	0.0176	0.0262

7. BEAM PATTERNS

To evaluate any large-scale errors of RT-16 reflector system, beam pattern measurements were carried out. Sensitivity of RT-16 is sufficient to measure first side lobes using bright astronomical sources, which can tell about feed, secondary mirror misalignments and large scale deformations of primary mirror. Automated raster scanning and data acquisition script was made for this purpose. In this case

'Z' type offset scanning was carried out while tracking the point source. Total power meter was used for signal registration in full ≈1200 MHz IF bandwidth of RHC channel. 3C405 was used as a point source, total measurement time for each pattern was about 30 minutes and during this time maximum antenna elevation change was about 5°. No amplitude calibration was done, so results were useable as rough estimate of beam shape. Measured (26 July, 2017) beam patterns at C1 and C4 sub-bands are shown in Fig. 9.

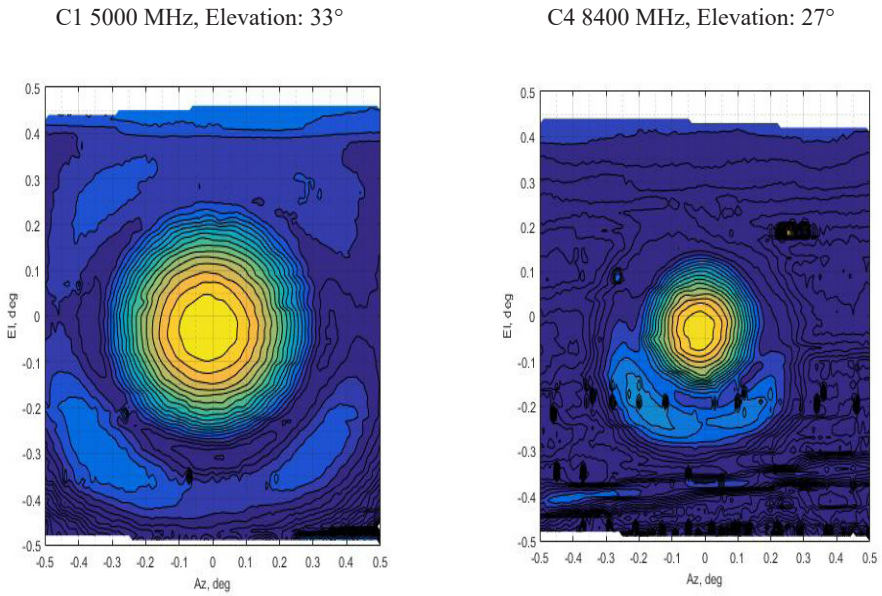

Fig. 9. Estimated beam patterns of RT-16 at C1 and C4 sub-bands.

Asymmetry of first side lobes are visible, which indicates lateral shift in secondary mirror or large-scale deformation of primary surface, of which last is very unlikely given the light, newly installed mirror structure. Increased amplitude in lower side of the beam indicates that secondary mirror may be laterally shifted downwards in elevation. In this case offset of the main lobe should be in positive Y direction – the shown patterns are centered on the main lobe due to a pointing model being applied during the measurements. It explains elevation dependent negative valued elevation offsets shown previously in this report and would mean that secondary mirror shift was dependent on elevation. Similarity of lobe shape in different elevations may indicate that there is a constant component of secondary shift present, which after correction could improve the performance even in case of elevation dependence. Concluding from gain curve measurements, influence of elevation dependent component of lateral shift on antenna gain is very small which is expected for small shifts relative to wavelength, but more rigorous tests should be carried out to better understand this issue. Main lobe width and side lobe offset is decreasing with increasing frequencies as it is expected. To increase the quality of measurements and allow comparing relative levels of side lobes with simulated values, amplitude calibration of the data must be carried out.

8. SUMMARY OF SENSITIVITY PERFORMANCE

Table 5 summarizes the sensitivity performance of RT-16 receiving system at different sub bands. DPFU and T_{sys} values are given in assumption that T_{cal} is known. Ratio of T_{sys} over DPFU or system effective flux density (SEFD) is a direct result from amplitude calibration source observations and should be more accurate. Gain relative to isotropic antenna and figure of merit values are derived from DFPU and SEFD measurements. The obtained efficiency values reasonably well match theoretically approximated values of 0.787 to 0.806 provided in manufacturer documentation of RT-16 [6]. Lower values may be explained with possible secondary mirror displacement, but it must be again verified after calibration of T_{cal}.

Table 5

Summary the RT-16 Sensitivity Performance

Sub band	Center freq, MHz	Pol	Tsys, K (Zenith)	DPFU, K/Jy (Max)	G, dBi (Max)	eff_A (Max)	SEFD, Jy (Zenith)	G/Tsys, dB (Zenith)
C1	**5000**	RCP	34.37	0.048	56.67	0.66	712.27	41.31
		LCP	29.89	0.056	57.32	0.77	533.34	42.37
C2	**6100**	RCP	28.79	0.052	58.71	0.71	556.14	44.11
		LCP	32.13	0.057	59.16	0.79	559.54	44.09
C3	**6700**	RCP	28.90	0.051	59.42	0.69	570.95	44.81
		LCP	31.38	0.055	59.81	0.76	567.31	44.84
C4	**8400**	RCP	29.27	0.043	60.65	0.59	684.90	45.99
		LCP	29.32	0.048	61.11	0.65	616.76	46.44

9. CONCLUSIONS

First overall performance evaluation of Irbene RT-16 radio telescope receiving system has been carried out, which may serve as a reference for future evaluation. Pointing calibration has been carried out to correct azimuth and elevation pointing errors to overall RMS of 54” and 23” respectively by employing the Field System pointing model. More efficient cross-scan algorithm should be implemented to allow for more uniform sky coverage of data in shorter period of time and utilization of weaker sources which will result in better accuracy of the current model. More rigorous characterization of azimuth offsets above elevations of 70° and azimuth offset dependence on direction of antenna slew must be carried out. Antenna gain measurements show relatively small dependence on elevation, which is expected. There is difference in both gain and system temperature values, which may be the result of insufficient knowledge of calibration noise diode temperature and should be verified after calibration of T_{cal}. Nevertheless, the gain curve coefficients and *Tcal[Jy]* ratios are measured for all four sub-bands of RT-16 receiver, which may serve for amplitude calibration of astronomical data. Beam pattern evaluation shows increased lower side lobe level which indicates possible lateral shift of secondary mirror. Given the large elevation dependent elevation offsets, it may be concluded

that secondary shift results from elevation dependent gradational influence on the secondary mirror. Overall measured figure of merit values in form of SEFD and G/T_{sys} are as expected considering the new high performance antenna and receiver and it is clear that apart from small mirror displacement no major performance limiting issues are present in the system.

REFERENCES

1. Himwich, W. E. (1993). NVI, Inc./GSFC, Antenna Calibration Programs - *VLBI Field System Documentation. NASA/Goddard Space Flight Center.*
2. Himwich, W. E. (1993). NVI, Inc./GSFC, Pointing Model Derivation - *VLBI Field System Documentation. NASA/Goddard Space Flight Center.*
3. Kraus, A. (2013). MPIfR, Calibration of Single Dish Telescopes. *ERATec Workshop, Bologna.*
4. Kraus, A. (2007). MPIfR. Calibration of the Effelsberg 100m telescope.
5. Perley, R. A., & Butler B. J. (2013). An Accurate Flux Density Scale from 1 to 50 GHz. *The Astrophysical Journal Supplement Series, DOI: 10.1088/0067-0049/204/2/19*
6. MT Mechatronics. (2015). *Report VTP2-DOC-11210-02: Assessment of the RT16 antenna surface performance and illumination efficiency.*

IRBENES RADIO TELESKOPA RT-16 UZTVEROŠĀS SISTĒMAS VEIKTSPĒJAS NOVĒRTĒJUMS

M. Bleiders, Vl. Bezrukovs, A. Orbidāns

K o p s a v i l k u m s

Šajā rakstā tiek prezentēti nesen renovētā Irbenes radioteleskopa RT-16 uztverošās sistēmas veiktspējas mērījumu rezultāti. Šī darba mērķis bija novērtēt RT-16 uztverošās sistēmas parametrus, kas ļautu veikt novērojumu datu amplitūdas kalibrēšanu vienas antenas un VLBI režīmos, uzlabot esošās sistēmas veiktspēju, kā arī monitorēt un salīdzināt veiktspēju iespējamu sistēmas izmaiņu gadījumā. Apskatītā uztverošā sistēma ir 16 m Kasegrēna tipa paraboliskā antena, kas aprīkota ar platjoslas kriogēni dzesēto uztvērēju ar frekvenču diapazonu no 4.5 līdz 8.8 GHz, kas sadalīts četrās apakš joslās. Ir veiktas virkne kalibrēšanas sesijas, novērojot astronomiskos avotus ar stabilu un zināmu intensitāti, izmantojot institūtā izstrādātu pilnās jaudas reģistratoru. Pirmkārt, tika veikti antenas stara pozicionēšanas nobīžu mērījumi, kas ļāva aprēķināt pozicionēšanas modeļa koeficientus. Pēc tam veikta amplitūdas kalibrācija, kas ietver teleskopa jutības, kalibrācijas trokšņu diodes ekvivalento intensitāti un pastiprinājuma līknes, veicot kalibrācijas avotu mērījumus dažādās antenas elevācijas pozīcijās. Papildus tam, novērtētas antenas virzības diagrammas visos četros frekvenču apakš diapazonos. Iegūtie rezultāti kalpos kā atskaites punkts, novērtējot RT-16 veiktspēju nākotnē.

10.11.2017.